

CDE-1 Affects Chromosome Segregation through Uridylation of CSR-1-Bound siRNAs

Josien C. van Wolfswinkel,^{1,2} Julie M. Claycomb,³ Pedro J. Batista,^{3,4} Craig C. Mello,^{3,5} Eugene Berezikov,¹ and René F. Ketting^{1,*}

¹Hubrecht Institute-KNAW and University Medical Centre Utrecht, Uppsalalaan 8, 3584 CT Utrecht, The Netherlands

²Department of Biomolecular Mass Spectrometry, Utrecht University, Sorbonnelaan 16, 3584 CA Utrecht, The Netherlands

³Program in Molecular Medicine, University of Massachusetts Medical School, Worcester, MA 01605, USA

⁴Gulbenkian PhD Programme in Biomedicine, Rua da Quinta Grande, 6, 2780-156, Oeiras, Portugal

⁵Howard Hughes Medical Institute, Worcester, MA 01605, USA

*Correspondence: r.ketting@hubrecht.eu

DOI 10.1016/j.cell.2009.09.012

SUMMARY

We have studied the function of a conserved germline-specific nucleotidyltransferase protein, CDE-1, in RNAi and chromosome segregation in *C. elegans*. CDE-1 localizes specifically to mitotic chromosomes in embryos. This localization requires the RdRP EGO-1, which physically interacts with CDE-1, and the Argonaute protein CSR-1. We found that CDE-1 is required for the uridylation of CSR-1 bound siRNAs, and that in the absence of CDE-1 these siRNAs accumulate to inappropriate levels, accompanied by defects in both meiotic and mitotic chromosome segregation. Elevated siRNA levels are associated with erroneous gene silencing, most likely through the inappropriate loading of CSR-1 siRNAs into other Argonaute proteins. We propose a model in which CDE-1 restricts specific EGO-1-generated siRNAs to the CSR-1 mediated, chromosome associated RNAi pathway, thus separating it from other endogenous RNAi pathways. The conserved nature of CDE-1 suggests that similar sorting mechanisms may operate in other animals, including mammals.

INTRODUCTION

RNA interference (RNAi) is an evolutionarily conserved mechanism in which genes are silenced by small RNA molecules (Fire et al., 1998; Mello and Conte, 2004). Genetic screens, in combination with biochemical studies, have elucidated the genes and mechanisms involved in the initiation and amplification of the RNAi response in *C. elegans*. Primary siRNAs are generated from long dsRNA via cleavage by DCR-1 and are incorporated in the RNA Induced Silencing Complex (RISC), whose main component is the Argonaute protein RDE-1. RISC is then targeted to an RNA molecule by sequence complementarity, marking this RNA for silencing. An RNA-directed RNA polymerase (RdRP) is then recruited and, using the targeted RNA as a template, synthesizes secondary siRNAs (Pak and Fire,

2007; Sijen et al., 2007). These secondary siRNAs are then loaded into RISCs containing any of a number of secondary, worm-specific Argonautes (WAGOs) (Yigit et al., 2006).

Several endogenous functions of the RNAi machinery in *C. elegans* have been described thus far. First, some genes involved in RNAi were found to be required for transposon silencing (Ketting et al., 1999; Tabara et al., 1999), and specific siRNAs derived from transposon sequences are thought to be causal to the silencing (Sijen and Plasterk, 2003). Second, several RNAi mutants show a *High incidence of males (Him)* phenotype (Ketting et al., 1999; Tabara et al., 1999), which often reflects an underlying defect in chromosome segregation. A direct role for RNAi components in this process has however not yet been demonstrated in animals.

Work in the fission yeast *Schizosaccharomyces pombe* has given a clear indication for a direct role of RNAi in genome stability. In *S. pombe*, RNAi is required for pericentromeric heterochromatin formation, and therefore for centromere function and faithful chromosome segregation (Hall et al., 2003; Martienssen et al., 2005). Two interacting protein complexes are involved in this mechanism. One is the RNA-Induced Transcriptional Silencing (RITS) complex, which consists of the Argonaute protein Ago1, the chromodomain protein Chp1, and the adaptor protein Tas3, and the other is the RNA-Directed RNAPolymerase Complex (RDRC), which contains the RNA-directed RNA polymerase Rdp1, the helicase Hrr1, and the nucleotidyltransferase Cid12 (Motamedi et al., 2004; Verdel et al., 2004). Both of these complexes are required to maintain silencing of pericentromeric repetitive sequences. Integrity of this pericentromeric heterochromatin is required both for the initial loading of the centromere-specific histone CENP-A (Folco et al., 2008) and for the establishment of a rigid structural framework of cohesins between the sister centromeres, to allow for bipolar spindle orientation and attachment (reviewed in Ekwall, 2004). Mutation of the nucleotidyltransferase Cid12 leads to increased errors in chromosome segregation due to premature loss of centromeric cohesion (Win et al., 2006).

In *C. elegans*, several family members of the Cid12 nucleotidyltransferase have been identified (Crittenden et al., 2003; Olsen et al., 2006; Schmid et al., 2009; Wang et al., 2002), of which *rde-3*, also known as *mut-2*, was shown to be involved in RNAi (Chen et al., 2005). In a previous screen for genes

involved in an RNAi-related silencing phenomenon named co-suppression (Robert et al., 2005), we identified *rde-3/mut-2* as well as two new family members: *cde-1* and *cde-2* (for cosuppression defective). *Cde-1* has since been named *cid-1* (for caffeine induced death) (Olsen et al., 2006) and *pup-1* (for poly(U) polymerase). However, *cde-1* mutant worms do not show a *cid* phenotype, nor does the name *pup-1* reveal any biological function, thus we prefer the name *cde-1*.

Here, we describe *cde-1* as a gene involved in RNAi and chromosome segregation. We place CDE-1 in a molecular pathway with the RdRP enzyme EGO-1 and the Argonaute CSR-1, with all three proteins localizing to chromosomes (also see Claycomb et al., 2009 [this issue of Cell]). CDE-1 uridylylates siRNAs generated in the context of the CSR-1 pathway, and loss of CDE-1 results in an increase of CSR-1 siRNA levels. This is accompanied by defects in chromosome segregation, much like those observed in *csr-1* mutants (Claycomb et al., 2009). We also present evidence that in *cde-1* mutants, siRNAs that are usually bound by CSR-1 now feed into other, CSR-1 independent RNAi pathways, including those mediating mRNA turnover. Thus, we propose that CDE-1 restricts siRNAs produced from specific loci by EGO-1 to one particular Argonaute, CSR-1, thereby playing a role in keeping the diverse RNAi pathways in *C. elegans* distinct and functionally separated from each other.

RESULTS

cde-1 Encodes a Conserved Nucleotidyltransferase with a Role in RNAi-Related Processes

The *cde-1* gene, K10D2.3, encodes a member of a larger protein family, often referred to as the TRF-like nucleotidyltransferases, with family members present from yeast to mammals (Figures 1A and 1B). CDE-1 has two TRF-like domains, of which only the more C-terminal one appears to be catalytically active, based on conservation of catalytic residues. We have raised an antibody against CDE-1 and have used that to immunopurify CDE-1 from *C. elegans* embryonic extracts and test its nucleotidyltransferase activity in vitro. In these assays, CDE-1 preferentially adds uridine nucleotides to the 3' end of a short RNA probe (Figure 1C), consistent with in vitro experiments using a recombinant CDE-1 fragment (Kwak and Wickens, 2007; Rissland et al., 2007). The activity displayed by CDE-1 is not very processive as indicated by the relatively short U-tails added to the substrate. Furthermore, the transferase activity is inhibited by the presence of a 2'O-methyl group on the most 3' nucleotide, a chemical modification found on some endogenous small RNA molecules (data not shown).

To study the role of *cde-1* in vivo we have used two deletion alleles (*tm1021* and *tm936*) (Figure 1B). Both alleles behave identically. *Cde-1* mutants do not display notable defects in general RNA metabolism, as judged by Northern blotting experiments for a number of noncoding RNAs (see Figure S1A available with this article online), but two endogenous siRNAs were slightly reduced in abundance (Figure S1B). Furthermore, both *cde-1* mutant alleles are fully sensitive to RNAi against somatically expressed genes but show reduced sensitivity to RNAi against germline genes (Figure 1D). It was previously reported that RNAi-mediated knockdown of *cde-1* relieves cosuppression

(Robert et al., 2005). We used the two *cde-1* alleles to confirm this phenotype (Figure 1E). Finally, we also tested the transposon activation phenotype described before by Robert et al. (Robert et al., 2005). Interestingly, upon testing Tc1 and Tc3 activity we found that only Tc1 becomes activated in the *cde-1* mutant background, and that this is accompanied by a loss of Tc1 specific siRNAs and by an increased load of double-stranded DNA breaks and apoptosis (Figures S2 and S3).

cde-1 Is Expressed in the Germline

We performed in situ hybridization to detect the localization of endogenous *cde-1* mRNA (Figure 2A). On whole mounts, clear staining of the gonad arms was visible and no other expression patterns were detected. Closer inspection on extruded gonads showed *cde-1* mRNA throughout the entire gonad, without clear localization to a specific region. Northern blot analysis showed that the *cde-1* signal was drastically decreased in the *glp-4(bn2)* mutant, which lacks a germline (Beanan and Strome, 1992) compared to wild-type worms, confirming its germline localization (Figure 2B). These results are consistent with *cde-1* expression data from previous microarray studies (Kim et al., 2001; Reinke et al., 2004; Reinke et al., 2000).

CDE-1 Localizes to Germline Granules and Embryonic Metaphase Plates

We used the antibodies raised against CDE-1 to examine its cellular and subcellular localization pattern throughout development. CDE-1 was detected throughout the female germline cytoplasm, where we found it to be enriched in the perinuclear region (Figure 2C). However, CDE-1 did not display the clear granular structure that is commonly observed for the P granule marker PGL-1 at this stage. In the sperm-producing germlines of both males and L4 stage hermaphrodites, bright granules were found in close proximity to the condensing DNA of maturing sperm. In embryos, CDE-1 was detected in perinuclear granules in the P-cell lineage, mainly colocalizing with PGL-1 (Figure 2D). In addition, staining could be detected on the outer edges of condensing chromosomes at prometaphase. This staining became more intense on the spindle-facing sides of the metaphase plate and remained detectable through anaphase (Figure 2E). Parallel experiments in *cde-1* mutant animals did not show the patterns described above (Figure S4), indicating that the observed signals reflect true CDE-1 localization. Specific intestinal staining as previously reported based on a transgenic approach (Olsen et al., 2006) could not be detected.

CDE-1 Affects Both Meiotic and Mitotic Chromosome Segregation

The brood of the *cde-1* mutant animals contains an increasing proportion of nonhatching eggs as animals age, ranging from 5% on the first day of adulthood to 80% on day 4 (data not shown). This is accompanied by an elevated percentage of males, suggesting that *cde-1* may affect chromosome segregation. We looked further into this embryonic viability phenotype using a number of assays. First, to evaluate the contribution of missegregation during mitosis in the germline we studied the chromosomal content of pachytene nuclei using Fluorescent In Situ Hybridization (FISH) with a probe against chromosome V.

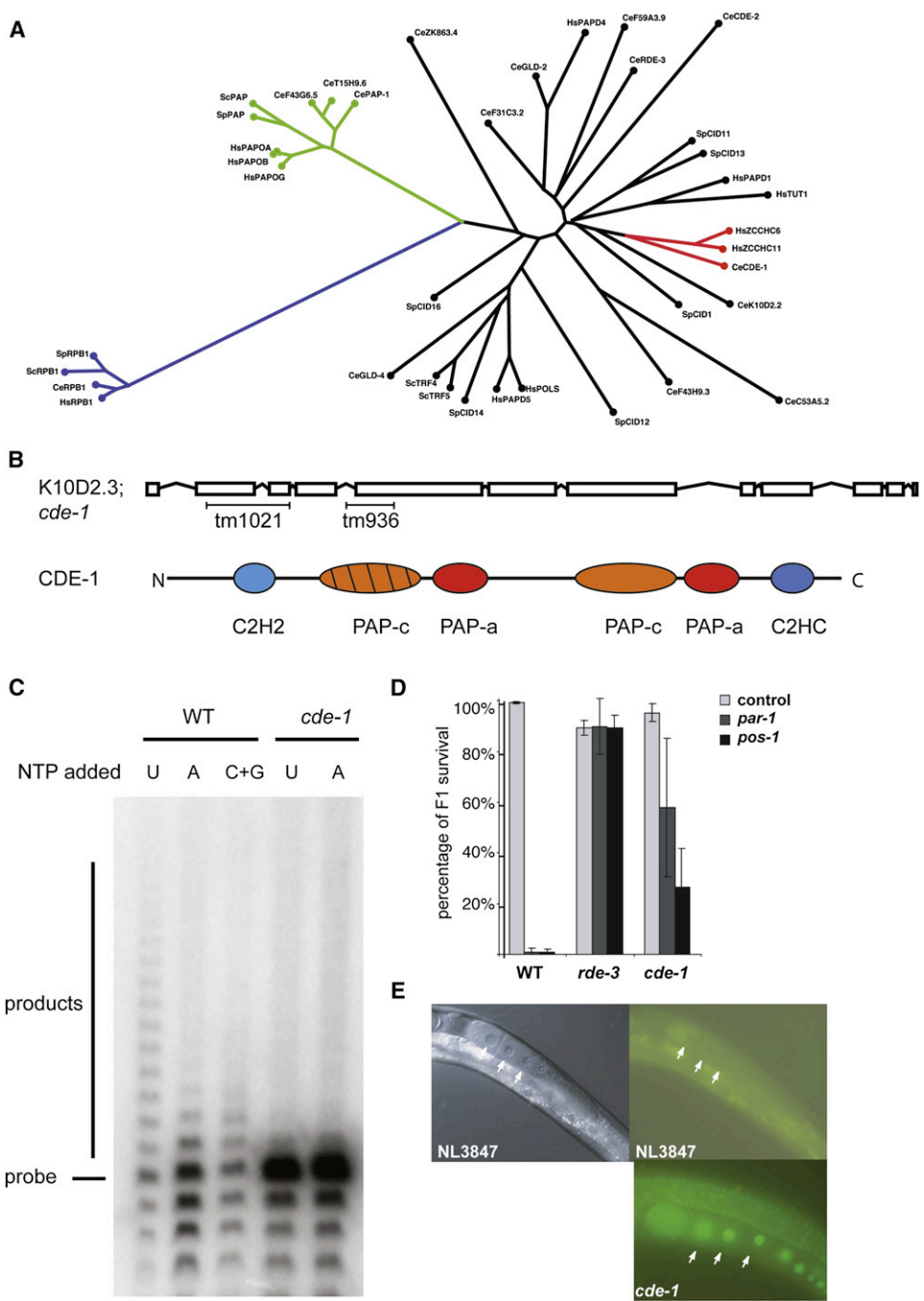


Figure 1. CDE-1 Is a Conserved Terminaltransferase Required for RNAi

(A) Phylogenetic tree displaying CDE-1 and other terminaltransferase proteins. Blue branch shows canonical RNA polymerases as an outgroup. In green canonical polyA polymerases are shown. The branch containing CDE-1 is shown in red.

(B) Schematic of the *cde-1* gene and CDE-1 protein. The two deletion alleles used in this study are indicated. *Tm1021* is located before the C2H2 domain and leads to a premature stop in the coding frame; *tm936* overlaps with the first PAP-c domain. The various protein domains found in CDE-1 are: Zn-Finger (C2H2); Zn-knuckle (C2HC); PolyA polymerase central domain (PAP-c; N-terminal PAP-c domain most likely is catalytically inactive); PAP associated domain (PAP-a).

(C) In vitro activity of immunopurified CDE-1. Immunoprecipitates from wild-type and *cde-1* mutant extracts were incubated with indicated radiolabelled RNA probe in the presence of different NTPs. Reaction products were run on a denaturing polyacrylamide gel.

(D) Bar diagram displaying RNAi sensitivities of wild-type and mutant *C. elegans* strains.

(E) Representative pictures visualizing defective *pie-1::gfp::H2B* silencing in *cde-1* mutant animals through cosuppression triggered by a repetitive array (nuclei indicated by white arrows).

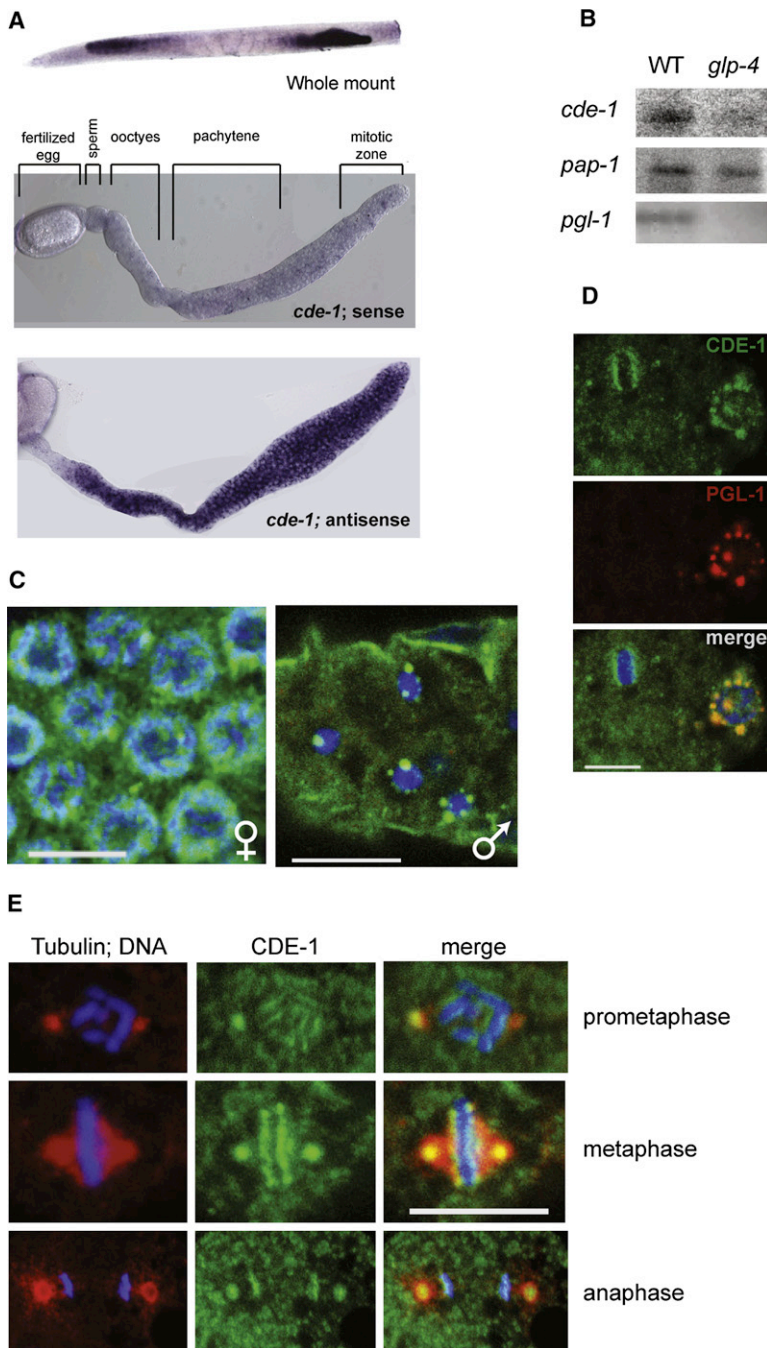


Figure 2. Expression of *cde-1*-Derived mRNA and Protein

(A) ISH of whole mount and extruded gonads with a probe anti-sense to *cde-1*. A sense probe was used as a control.

(B) Northern blot for *cde-1* mRNA in wild-type and *glp-4(bn2)* mutant (germline-less) animals. The ubiquitously expressed poly(A) polymerase *pap-1* and germline specific *pgl-1* genes were used as a controls.

(C) CDE-1 protein is present in both female and male germlines. Germlines were stained with CDE-1 antiserum (green) and DAPI (blue). Shown images are single sections acquired by confocal microscopy. The scale bar represents 5 μ m.

(D) CDE-1 is present in P-granules in the early embryo. Embryos were costained with CDE-1 antiserum (green), antibody against P-granule protein PGL-1 (red), and DAPI (blue). Shown images are single sections acquired by confocal microscopy. The scale bar represents 5 μ m.

(E) CDE-1 is on chromosomes at prometaphase, metaphase and anaphase. Embryos were costained for CDE-1 (green), DNA (DAPI; blue) and against tubulin (red). The scale bar represents 5 μ m.

Third, we used SNP typing to characterize the gross chromosomal makeup of 104 nonhatching eggs that resulted from a cross between *cde-1* and males of a Hawaiian strain of *C. elegans*. (For a detailed description and additional controls see Supplemental Results and Figure S5). In 29% of the dead embryos, abnormal underrepresentation of one or more chromosomes was detected (Figure 3B). In 46% of those embryos, abnormalities involved more than one chromosome, indicating a major segregation failure. Both Bristol copies and Hawaiian copies were affected (Figure S5A).

The fact that not only N2-derived chromosomes, but also Hawaiian-derived chromosomes were affected by *cde-1* mutation, suggests that at least part of the missegregation occurs during embryonic mitosis. In order to find cytological indications for embryonic missegregation, we stained early embryos for DNA and microtubules. In early embryos of *cde-1* mutants grown at 25°C several aberrant segregation figures were identified (Figure S6). Bridging DNA at anaphase was frequently detected, and occasionally severe spindle defects such as a tripolar spindle were observed.

Aberrant chromosome segregation during embryonic cell division was confirmed by FISH on early embryos with probes against chromosome V:

out of 32 wild-type 2-12 cell embryos only 2 showed aberrant segregation, whereas 23 aberrant segregation patterns were found among 36 *cde-1* mutant embryos (Figure 3C).

We next used video microscopy to visualize the first embryonic divisions in real time. Still frames from representative movies (Movies S1–S3) are shown in Figure 3D. Two major defects were identified in the *cde-1* embryos from aged mothers. First, bridging DNA at anaphase was frequently observed. Although mitosis was carried to completion in all cases, chromosome bridging was present throughout anaphase, resulting in

Among 500 *cde-1* nuclei analyzed, no aberrations were detected, indicating that mitotic germline missegregation is rare (data not shown).

Next, we analyzed the chromosomes in diakinetid oocytes using regular DAPI staining. This revealed that in *cde-1* mutants frequently one or more bivalents separated into univalents (Figures 3A, S3D, and S3E), most likely causing the observed Him phenotype in the *cde-1* mutant. This indicates that the pairing of homologous chromosomes during meiosis is affected by CDE-1.

two daughter nuclei that remained connected to each other by DNA strands (Figure 3E middle panel). Upon cytokinesis these strands were broken, resulting in a seemingly normal 2-cell embryo, although some DNA was probably lost during this division. The second defect concerned extrusion of the second polar body. In several of the subsequent divisions, the second polar body remained present in the cytoplasm, and could therefore join the pronuclei in the division (Figure 3E, right panel). We note that this type of meiotic defect will influence the read-out in some of the above-mentioned experiments, which analyze paternal and maternal chromosomes at the same time. Therefore we repeated the FISH analysis using probes against an integrated transgenic locus that was crossed in via a wild-type male (Figure 3D). This showed clear evidence of mitotic defects in embryos derived from *cde-1* mutant mothers, but not in those derived from wild-type mothers.

Chromosome Alignment Defects in *cde-1* Mutants

To further evaluate the function of CDE-1 in mitosis we studied the localization of centromeric histone protein CENP-A and outer kinetochore protein CENP-F using immunohistochemistry. In wild-type embryos these proteins localize in what appear to be parallel lines on the spindle facing sides of the metaphase plate (Figure 3F) (Buchwitz et al., 1999). In *cde-1* mutants, CENP-A loaded normally onto chromosomes at prometaphase (Figure S7A), and formed clear concentrations at metaphase. However, frequently CENP-A did not form straight lines along the metaphase plate. Instead, CENP-A appeared interrupted, with connections between the two faces of the plate, or was “striped,” with many lines of CENP-A in parallel, resulting in a twisted appearance of the metaphase plate. Staining of the outer kinetochore protein CENP-F (Moore et al., 1999) confirmed the notion that the metaphase plate is disorganized in *cde-1* (Figure S7B).

To analyze the metaphase plate defects in more detail we followed formation and separation of the metaphase plate in real time using GFP::KBP-4 as a kinetochore marker (Gassmann et al., 2008). KBP-4 begins to flank opposite faces of the chromosomes during prophase, and rapidly becomes visible as two distinct lines on the spindle-facing sides of the metaphase plate as the result of chromosome alignment. As shown in Figure 3G, in absence of CDE-1, KBP-4 loads normally onto chromosomes, at least at the resolution of our current analysis. However, CDE-1 appears to be required for efficient alignment of the chromosomes at the metaphase plate, as mutant embryos often go into anaphase when chromosomes have not yet fully aligned. This is consistent with our finding that the disorganized metaphase plates observed using immunohistochemistry were also observed in wild-type embryos, albeit at a much lower frequency (Figures 3F and S7B), suggesting that the disorganized state of the metaphase plate also occurs in wild-type animals, but becomes more rapidly organized compared to metaphase plates in *cde-1* mutants.

CDE-1 Localization Requires EGO-1 and CSR-1

In fission yeast, the nucleotidyltransferase protein Cid12 associates with the RdRP enzyme Rdp1. In turn this complex interacts with the Argonaute protein Ago1 (Motamedi et al., 2004). For various reasons, EGO-1 (an RdRP) and CSR-1 (an Argonaute)

are *C. elegans* candidates to interact with CDE-1 in a similar manner. First, EGO-1 and CSR-1 show localization to and around the metaphase plate (Claycomb et al., 2009), much like that of CDE-1. Second, *csr-1* is one of three Argonaute genes that had been identified in the cosuppression screen in which also *cde-1* was identified (Robert et al., 2005). Third, mutations in *csr-1* and *ego-1* also lead to defects in CENP-A localization and chromosome segregation (Figure S7C) (Claycomb et al., 2009; Smardon et al., 2000; Yigit et al., 2006). We therefore asked whether CDE-1 interacts with EGO-1 and CSR-1.

First we asked whether subcellular localization of CDE-1 depends on EGO-1 and CSR-1. We used RNAi in an RNAi hypersensitive genetic background (*rrf-3* mutant) to knock down *ego-1* and *csr-1*. In *rrf-3* mutant embryos, CDE-1 localized to the outside of the metaphase plate, just as in wild-type embryos. After RNAi against *ego-1*, CDE-1 localization was dispersed over the whole plate (Figure 4A). The granular structures found on condensing sperm DNA were no longer detectable, but instead a halo around the DNA was formed. On the other hand, RNAi against *csr-1* resulted in very faint (but correct) or no localization of CDE-1 to the metaphase plate. Sperm granules still contained CDE-1 after *csr-1* knock-down, but these granules did not associate with the condensing DNA anymore (Figure 4A). P-granule localization of CDE-1 was not affected by knock-down of either *ego-1* or *csr-1* (data not shown). EGO-1 and CSR-1 localization in absence of CDE-1 appears to be largely normal (data not shown).

To test whether CDE-1, EGO-1 and CSR-1 physically interact we performed co-immunoprecipitation experiments (Figure 4B). Using antibodies specific for CDE-1 we were able to pull down EGO-1, but not CSR-1 (not shown), from embryonic extracts. EGO-1 did not come down from *cde-1* mutant extracts, while EGO-1 levels were normal. These results strongly suggest that CDE-1 and EGO-1 are present in a shared complex.

Uridylation by CDE-1 Affects siRNA Accumulation

We used deep sequencing of wild-type and *cde-1* mutant small RNA libraries to gain further insights in the role of CDE-1 in small RNA metabolism. More than 5 million reads were obtained from each library (Table S2). To analyze the data, we first removed all reads derived from structural RNAs like rRNAs and tRNAs. Then, we defined five classes of (potential) genuine RNAi related small RNAs: siRNAs (antisense to coding regions), miRNAs, 21U RNAs, repeat derived small RNAs and “other” (see Supplemental Data). The sixth class, sense RNAs, most likely represents mRNA degradation products (Supplemental Experimental Procedures and Figure S10). Comparison of the libraries showed that in the *cde-1* mutant, the relative contribution of reads that match miRNAs is mildly reduced, whereas the fractions of repeat derived small RNAs and 21U RNAs remain unaltered. Most notably, the fraction of siRNAs is much increased (Figures 5A and S8). The genes matching these extra siRNAs are distributed evenly throughout the genome (Figure 5B).

As siRNA levels are increased in the *cde-1* mutant, and as CDE-1 is a nucleotidyltransferase that catalyzes 3' uridylation, a mark associated with miRNA degradation in plants (Li et al., 2005), we asked whether siRNAs carried any specific 3' nontemplated bases, in particular uracils. These should be apparent in

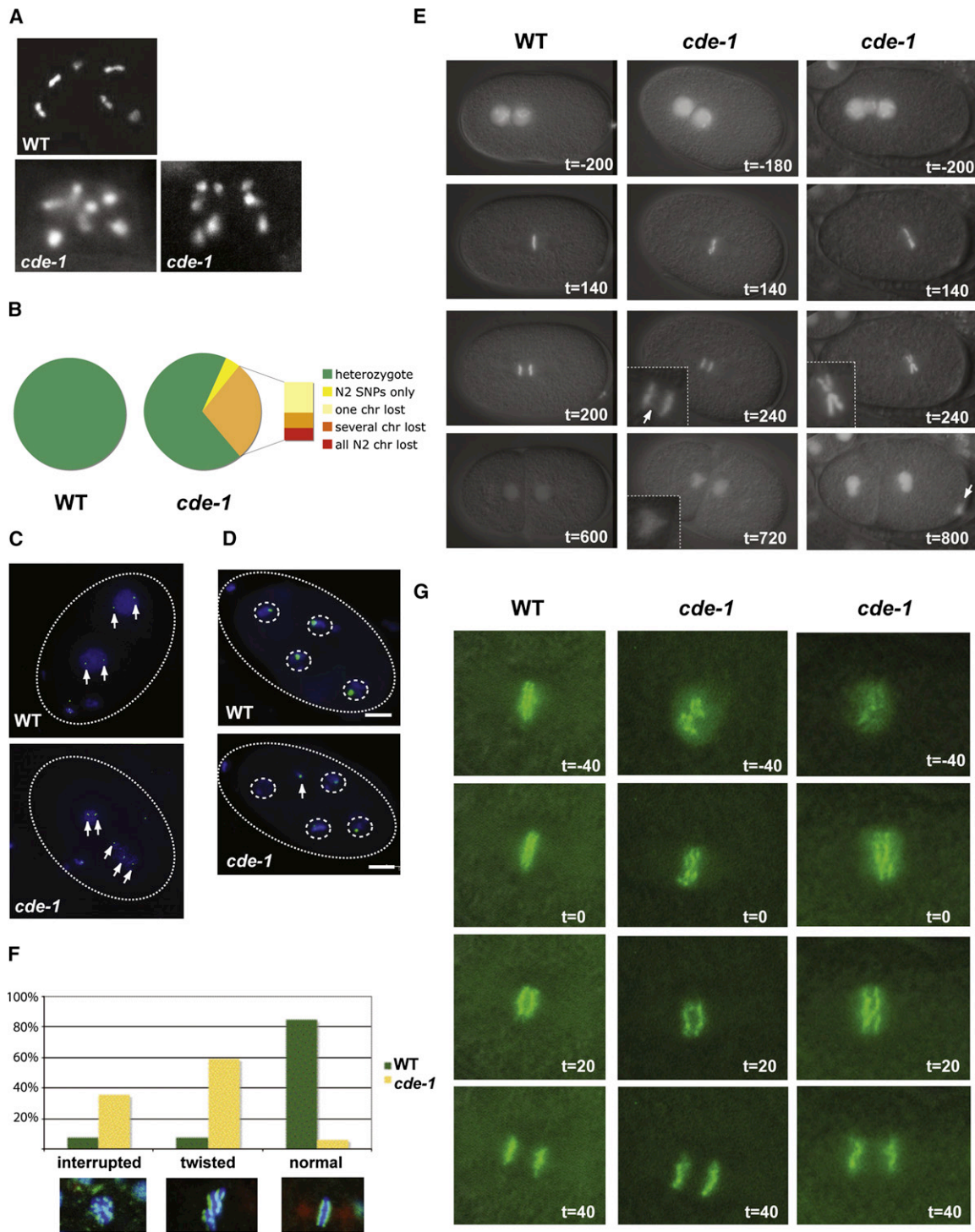


Figure 3. Chromosome Missegregation in *cde-1* Mutants

(A) Bivalents in *cde-1* oocytes are abnormal. Shown are images of DAPI-stained diakinetic oocytes.

(B) SNP analysis of embryos making use of the high frequency of SNPs between the wild-type strain N2 and CB4856. Pie charts show the extent of chromosomal loss in these embryos. Green indicates both male and female copies are present in equal quantities. Other colors indicate one or more chromosomes are under-represented. Per strain, at least 100 embryos were analyzed.

(C) Fluorescent ISH with probes against chromosome V (green) shows aberrant segregation patterns in *cde-1*. Images show projections of z-stacks through the entire embryo, after deconvolution. Dotted lines indicate embryo outlines. Arrows indicate individual loci stained.

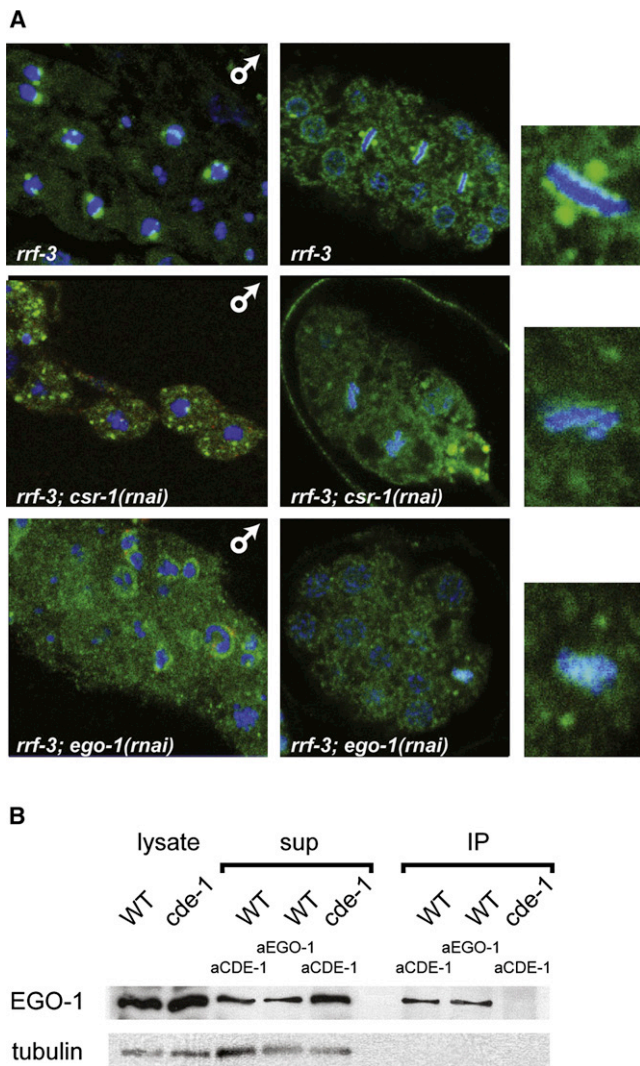


Figure 4. CDE-1 Interacts with EGO-1 and CSR-1

(A) CDE-1 localization in *rrf-3* RNAi hypersensitive animals, after RNAi against a nonendogenous control sequence, *ego-1* or *csr-1*.

(B) Immunoprecipitation of CDE-1 followed by western blot analysis probing for EGO-1.

the library sequences as additional thymidines that do not match the genome. We found that in wild-type libraries a major fraction of siRNA reads, but not miRNA reads, indeed has such extra thymidines, and that these are absent in libraries derived from three-day old *cde-1* mutant adults (Figure 5C). Interestingly, nontemplated thymidines were still present on siRNA reads derived

from *cde-1* mutant adults right after the last molt (data not shown), a time point when the *cde-1* mutant phenotype is still weak. We interpret this as meaning that an activity redundant with CDE-1 is present in young adults and not in older animals (see Discussion). The average length of the U tails added to siRNAs is very short (Figure 5D). This is consistent with our finding that immunopurified CDE-1 protein has low processivity (Figure 1C).

When we plot the total number of siRNA reads per gene versus the number of reads that carry extra thymidine bases, we find two populations of genes: a population of which siRNAs frequently carry nontemplated Ts (high T-trim) and a population in which this is much less frequent (low T-trim) (Figure 5E). The siRNA levels derived from high- and low-T-trim populations strongly correlate with the extent to which they are affected by loss of CDE-1: siRNAs derived from the high T-trim population increased in abundance in the *cde-1* mutant, whereas those derived from the low T-trim population did not react (Figure 5F). These data strongly suggest that a subset of siRNAs is uridylylated in vivo by CDE-1 and that this uridylation results in destabilization of those siRNAs.

CSR-1-Bound siRNAs Are Uridylylated by CDE-1

Genes matching the high T-trim population significantly overlap with CSR-1 targets (Figure 6A; Claycomb et al., 2009). In contrast, the low T-trim population is almost devoid of CSR-1 targets. This indicates that uridylation of siRNAs is not a widespread phenomenon, but that it is largely restricted to RNAi pathways involving CSR-1. We asked whether the uridylylated siRNAs could represent specimens that are not yet, or not anymore bound to CSR-1. As shown in Figure 6B, siRNAs cloned from CSR-1 immunoprecipitates derived from wild-type animals show levels of uridylation comparable with those observed in the total small RNA library. Furthermore, this uridylation depends on CDE-1, demonstrating that uridylylated siRNAs are physically bound by CSR-1. Uridylation is not a requirement for siRNAs to bind to CSR-1 as more than 60% of the CSR-1 bound siRNA reads that lacked nontemplated bases at their 3' ends terminated with a G, C or A (data not shown).

In the absence of CDE-1, CSR-1 still preferentially binds to siRNAs (Figure 6C). Also the identity of the genes represented by these siRNAs and their relative frequencies remain mostly unchanged (Figure S9). However, the ratio between siRNAs and other small RNA species, which most likely nonspecifically come down during the IP and are retained by the cloning method used, increases significantly. Most likely, these results reflect a difference in CSR-1 occupation by siRNAs between wild-type and *cde-1* mutant animals, with the CSR-1 protein pool being more extensively loaded when CDE-1 is not present.

(D) FISH with a probe against an integrated transgene that was crossed into the embryo from male sperm. No defects were observed in 33 wild-type embryos, whereas 9 out of 104 *cde-1* mutant embryos showed clear defects.

(E) Time-lapse microscopy of embryos expressing HIS2B::GFP in a wild-type (left) or *cde-1* (middle and right) background. Numbers indicate time in seconds relative to Nuclear Envelope BreakDown (NEBD). The movies from which these stills are captured, are provided in the Supplemental Data. The arrow at t = 240 in the middle panel indicates chromatin threads in between the two separating DNA plates. Arrow at t = 800 indicates polar body.

(F) Quantification of CENPA metaphase figures in wild-type and *cde-1* mutants.

(G) Stills from a time-lapse experiment using KBP-4::GFP to visualize the kinetochore. Frames were recorded every 20 s, with t = 0 s being the last frame before anaphase. Full movies are available in the Supplemental Data (Movies S4, S5, and S6).

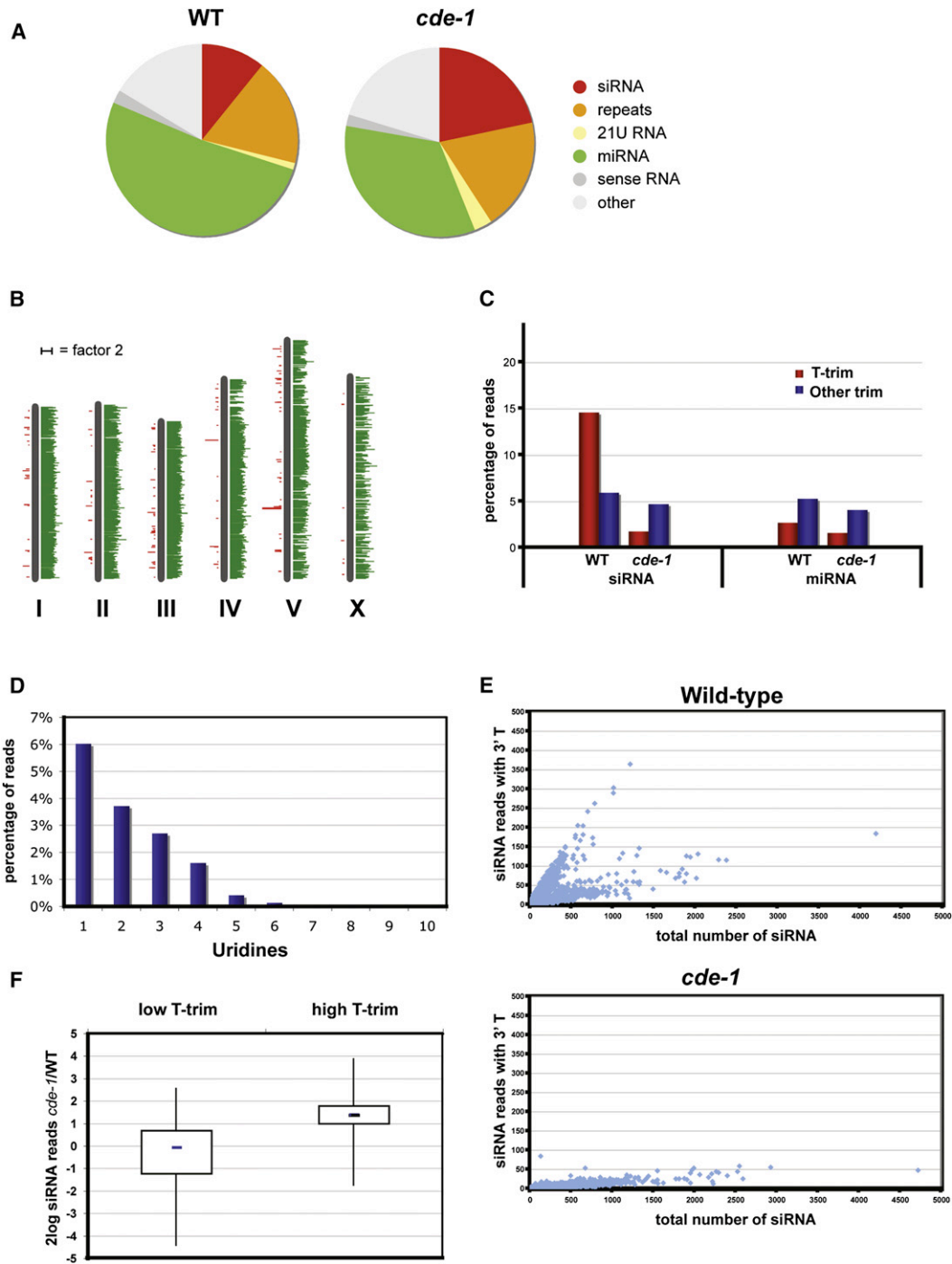


Figure 5. Uridylation of siRNAs In Vivo by CDE-1

(A) Pie charts showing the various small RNA populations in wild-type and *cde-1* mutant animals. Structural RNA reads were not included. (B) Libraries were normalized to miRNAs, and the 2log of the ratio between the normalized siRNA reads in the *cde-1* mutant versus the reads in the wild-type library were plotted. Green bars to the right show positive 2log values (higher number of reads in the *cde-1* mutant library). Red bars on the left show negative 2log values. (C) Bar diagram displaying the percentage of reads that required trimming at the 3' end of the read. Two types of trims were defined: T-only trims and other trims. (D) Length distribution of U tails on siRNAs. y axis displays percentage of total siRNA reads. (E) Scatter plot in which the number of siRNAs matching to a given gene was plotted versus the amount of siRNAs from that gene that required 3' end T trimming. Upper plot shows wild-type, lower plot *cde-1* mutant distribution. (F) Box plot showing differential response of siRNAs from high T-trim genes and low T-trim genes to loss of CDE-1. Blue line indicates the median, the box represents the middle 50% of the values and the lines show the maximum range of values.

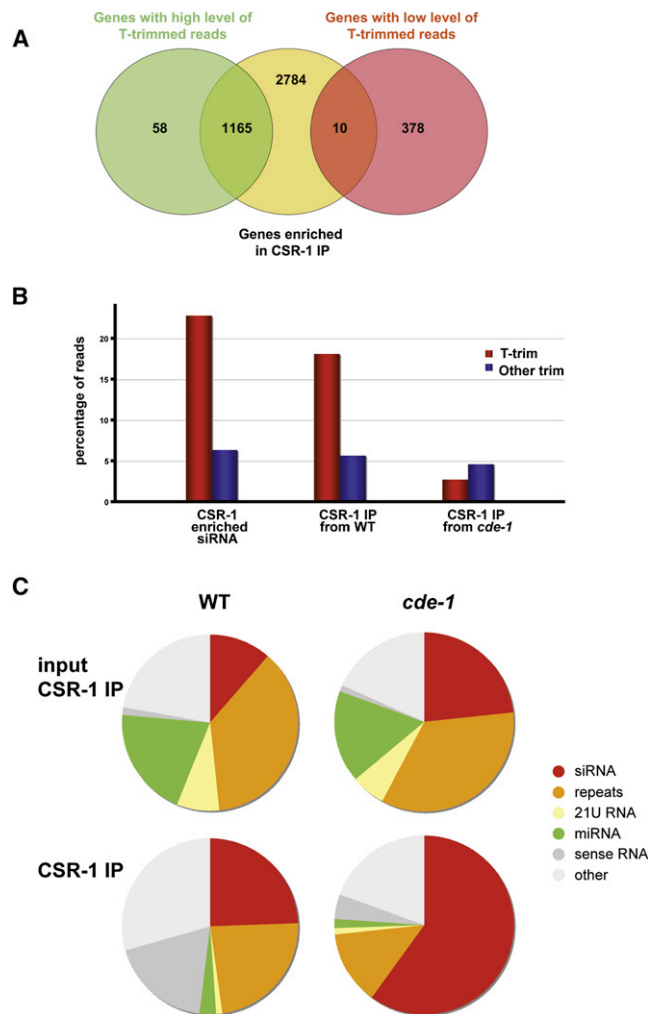


Figure 6. CDE-1 Modifies CSR-1-Bound siRNAs

(A) Venn diagram showing the overlap between high T-trim genes, low T-trim genes and CSR-1 target genes.

(B) Bar diagram comparing T-trimming of presumed CSR-1 associated siRNAs as they were identified computationally from total RNA libraries (left panel) and as they were physically pulled down with CSR-1 antibodies from wild-type and *cde-1* mutant animals (middle and right panel).

(C) Pie-charts showing small RNAs, split into different groups, cloned from wild-type and *cde-1* mutant extracts (input) and CSR-1 immunoprecipitates (CSR-1 IP).

Ectopic siRNA Effects in *cde-1* Mutants

Based on the data provided we propose a model in which CDE-1 uridylylates siRNAs that will be, or have been loaded into CSR-1. Without this uridylation these siRNAs accumulate to inappropriate levels, causing CSR-1 to function improperly (Figure 7A). A prediction of this model is that some siRNAs may start to flow into different RNAi pathways, mediated by different Argonaute proteins. To address this we looked at effects of *cde-1* mutation on mRNA levels using microarray analysis in relation to the observed changes in siRNA levels, as at least some endogenous RNAi pathways downregulate mRNA levels. As CSR-1 is not involved in regulating mRNA levels (Claycomb et al., 2009)

this could reflect spreading of normally CSR-1 bound siRNAs into another RNAi pathway. Indeed, using total RNA isolated from wild-type and *cde-1* mutant gonads, we find that more genes are downregulated than upregulated in the *cde-1* mutant germline (Table S1), and that there is a significant correlation between the increase in siRNA coverage of a given gene and the decrease in mRNA levels of that gene in the *cde-1* mutant (Figure 7B). We performed the same analysis but now comparing siRNAs specifically interacting with CSR-1 in either wild-type or *cde-1* mutant backgrounds (Figure 7B). In this case we do not observe a significant correlation between changes in siRNA coverage and gene expression, suggesting that CSR-1 is not responsible for the observed gene silencing effects in *cde-1* mutants.

DISCUSSION

It was previously reported that CDE-1 is required for efficient germline RNAi (Robert et al., 2005). We now show that CDE-1 destabilizes endogenous siRNAs in one particular RNAi pathway, the CSR-1 pathway, and that loss of CDE-1 results in a mitotic chromosome alignment defect. Furthermore, the data suggest that other RNAi pathways are also affected by the absence of CDE-1, leading to secondary effects. These secondary effects include less efficient transposon silencing, possibly through transposon siRNAs being competed by other siRNAs, and reduced expression of genes targeted by inappropriately accumulated siRNAs. Transposon silencing defects in *cde-1* mutants are discussed further in the Supplementary text; here we will focus on the biochemical activities of CDE-1 and its role in RNAi, in particular in relation to the Argonaute protein CSR-1 and chromosome segregation.

cde-1 and RNAi

Deep sequencing analysis of wild-type and *cde-1* mutant small RNAs revealed that the proportion of small RNA reads that map to genes is increased in the *cde-1* mutant. Interestingly, when compared to wild-type, small RNAs of antisense (siRNAs) rather than those of sense polarity (which we largely regard as nonspecific, see Supplemental discussion) were increased. Moreover, we observed a preferential enrichment for siRNAs covering genes with low siRNA coverage in wild-type. Although the magnitude of these effects was variable, the trend was reflected in three independent sets of libraries. In contrast, miRNA levels changed only slightly in *cde-1* compared to wild-type, and ratios between individual miRNA reads were maintained. This specific increase in siRNA reads could indicate an overactive secondary siRNA response, as thought to be mediated by RNA dependent RNA polymerases (RdRPs).

The increase in siRNAs in the *cde-1* deep sequencing libraries seems contradictory to the decrease of two endogenous siRNAs as detected by Northern blot (Figure S1B). However, although the total number of siRNAs is increased in the *cde-1* mutant, the number of reads of most individual siRNAs is reduced. The increased siRNA load may therefore also explain the reduced sensitivity of the *cde-1* mutant to exogenous RNAi. As the exogenously introduced siRNAs have to compete for the silencing machinery with all endogenous siRNAs present, and as the

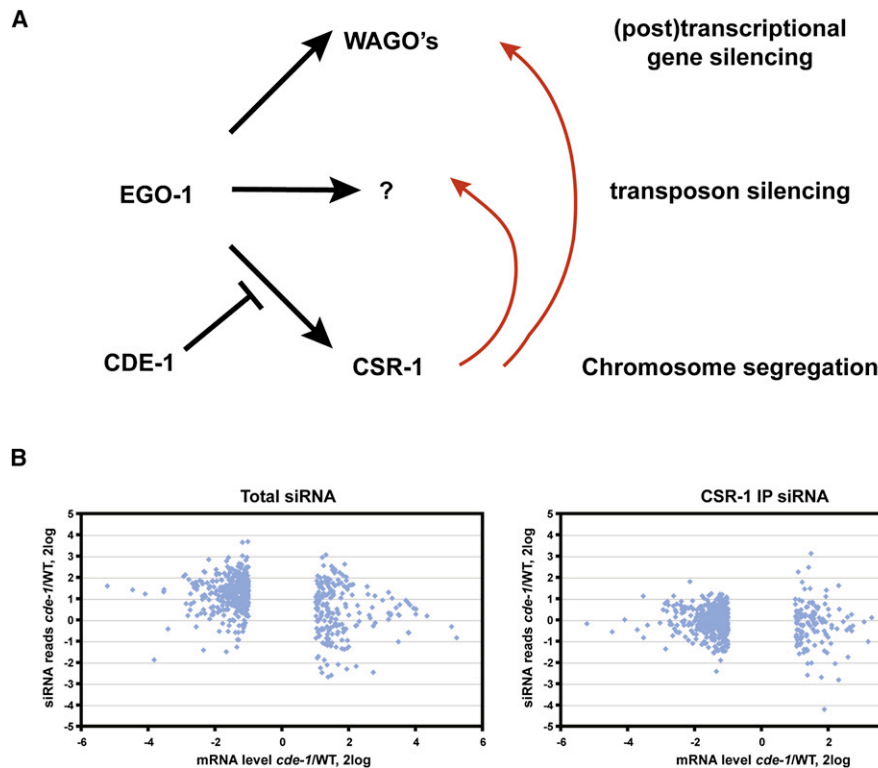


Figure 7. A Model for CDE-1 Activity in *C. elegans*

(A) Schematic model of CDE-1 activity in the CSR-1 pathway, and how defective CDE-1 may affect other RNAi pathways as well. Our data strongly suggest that CDE-1 limits the accumulation of siRNAs in the CSR-1 RNAi pathway. When CDE-1 is not present, these siRNAs accumulate to high levels and may start to spread into parallel RNAi pathways mediated by different Argonaute proteins (red arrows).

(B) Correlation between siRNA coverage and mRNA levels in wild-type and *cde-1* mutant gonads. siRNA read numbers for each gene were normalized to the size of the siRNA class. The x axis shows the 2log values of the mRNA ratios in the *cde-1* mutant and the wild-type, as determined by microarray analysis. Only genes that were significantly upregulated or significantly downregulated (factor > 2, $p < 0.05$) are included. y axis shows the 2log of the ratio between the normalized siRNA reads in the *cde-1* mutant and the reads in the wild-type library. Shown are only genes for which more than 10 reads in each library were identified. Comparison of the two populations showed a significant increase in siRNA reads for genes that were downregulated in the microarray ($p < 0.0001$).

pool of endogenous siRNAs is much enlarged, the efficiency of exogenous RNAi will be diminished.

Increases in endogenous siRNA levels in the *cde-1* mutant are functional, in the sense that they correspond to gene silencing effects on the mRNA level, as determined by microarray analysis. However, CSR-1, although previously shown to act as a slicer directed by secondary siRNAs (Aoki et al., 2007), appears not to be involved in this aberrant gene silencing (Figure 7B and manuscript by Claycomb et al., 2009). Our hypothesis is that another Argonaute is responsible for these observed gene silencing effects, implying that CDE-1 may effectively act to keep different endogenous RNAi-related pathways separate (also see Discussion Gu et al., 2009 and the paragraph below).

Biochemical Activity of CDE-1

In vitro studies on the catalytic activity of recombinant nucleotidyltransferases have shown that CDE-1 preferentially modifies RNA molecules by the attachment of uracil nucleotides to the 3' end (Kwak and Wickens, 2007). Our in vitro assay using immunopurified CDE-1 from *C. elegans* embryos confirms this finding and in addition shows that the enzyme is not very processive. Until now it was not clear what the in vivo targets of CDE-1

were and what the effect of CDE-1 activity would be. CDE-1 could modify long transcripts from specific genomic regions to mark them for further processing. These processing events could for example lead to degradation or stabilization, although uridylation is generally considered a destabilizing mark (see for example Heo et al., 2008 and Risland and Norbury, 2009). Such a requirement for nucleotidyltransferase activity has been reported before in *S. pombe*, where CID14 destabilizes rRNA and tRNA through uridylation in order to prevent them from entering the RNAi pathway (Buhler et al., 2008). However, the direct interaction we observe between CDE-1 and EGO-1 and our observations on 3' end uridylation of CSR-1 bound siRNAs both argue against such a scenario and support a model in which the substrates of CDE-1 are siRNAs. In plants it has been shown that miRNAs with an unprotected 3' end become uridylated and destabilized (Li et al., 2005). Our results are consistent with a similar role for CDE-1 in modifying, and subsequently destabilizing siRNAs made by EGO-1 in the context of the CSR-1 pathway (Figure 7A).

At present we can only speculate why such a control of siRNA abundance would be required. One explanation may be that siRNAs from the CSR-1 pathway are detrimental when

erroneously entered into other RNAi pathways, and are therefore kept at low concentrations. Consistent with this idea is the finding by Claycomb et al., 2009 that CSR-1 bound siRNAs are rare in comparison to siRNAs from other RNAi pathways (also see paper by Gu et al., 2009). Interference of CSR-1 siRNAs with other RNAi pathways may be exemplified by the reduced exogenous RNAi potency and relaxed transposon silencing in *cde-1* mutants. In addition, erroneous incorporation of CSR-1 siRNAs in other RNAi pathways may lead to inappropriate activity of these RNAi pathways at locations where CSR-1 should only be active. In this view, CDE-1, and perhaps other nucleotidyltransferases, may be regarded as factors required for adequate separation of different RNAi pathways, or perhaps even as siRNA sorting factors.

Another, not mutually exclusive possibility is that CSR-1 needs to be loaded in a flexible manner, as evidenced by our finding that CSR-1 immunoprecipitates contain many more siRNA molecules in *cde-1* mutant compared to wild-type animals, suggesting that CSR-1 in a normal situation is only partially loaded with siRNAs. This could relate to the above suggested deleterious effects of CSR-1 siRNAs in other pathways by making sure that there is always unloaded CSR-1 protein available to accept newly made siRNAs, but also to some unknown, intrinsic property of the CSR-1 pathway itself, which requires that the half-life of siRNAs in complex with CSR-1 is actively reduced through the action of CDE-1.

Redundancy

Clearly, embryonic lethality in *ego-1* and *csr-1* mutants is more severe than in *cde-1*. One cause behind the relatively mild *cde-1* phenotype could be redundancy, as there are eleven CID12 family members in *C. elegans*, three of which (*cde-1*, *cde-2* and *rde-3*) are known to be involved in RNAi-like processes. Gu et al., 2009 show that *rde-3* is involved in a branch of the endo siRNA mechanism that produces siRNAs that are depleted from CSR-1. CDE-1 and RDE-3 therefore seem to function in parallel pathways, that involve different Argonaute proteins targeting largely nonoverlapping RNAs.

Interestingly, the *cde-1 rde-3* double mutant shows a much stronger phenotype than either of the single mutants. Whereas both single mutants are viable, the double mutant shows a very penetrant deterioration of the germline and remains grandchild-less (Figure S11). Whether this is the result of truly complementing activities between CDE-1 and RDE-3 or of crippling two endogenous RNAi pathways at the same time requires further experimentation, but the results described by Gu et al., 2009 seem to favor the latter explanation.

In contrast to CDE-1, loss of RDE-3 induces a loss of siRNAs (Gu et al., 2009), suggesting a stabilizing role for RDE-3. Interestingly, RDE-3 clusters in a branch of nucleotidyltransferase proteins of which another member, GLD-2, has been shown to adenylate its target (Figure 1A). In fact, in a recent paper it was shown that the mouse GLD-2 protein stabilizes miR122 by 3' adenylation (Kato et al., 2009). Alternatively, as no catalytic activity was found for recombinant RDE-3 in vitro (Kwak and Wickens, 2007), a function of RDE-3 may be to compete with other, active, nucleotidyltransferases like CDE-1, thereby preventing destabilization of siRNAs. Related to this it is interesting to note that the

conserved N-terminal polymerase domain of CDE-1 is also presumably inactive, due to mutations in the conserved catalytic residues, suggesting a wider function for such inactive nucleotidyltransferase domains.

Finally, redundancy may also be seen in the fact that the severity of the *cde-1* mutant phenotype is age dependent. At young age chromosomal missegregation is weak, few double strand breaks are detectable in the germline, and siRNA-uridylation still occurs. This is not due to maternal contribution of *cde-1* gene products, as the strain is kept in a homozygous mutant state. Possibly, in young animals another nucleotidyltransferase is at least partially redundant with CDE-1, while in older animals this activity is no longer present.

RITS and RDRC in *C. elegans*?

In *S. pombe* the nucleotidyltransferase protein Cid12 has been found in physical association with the *S. pombe* homolog of EGO-1, Rdp1, and with the *S. pombe* Argonaute Ago1. We find that CDE-1 associates with EGO-1 and that proper subcellular localization of CDE-1 requires CSR-1. All three proteins display a CENP-A-like localization on chromosomes and are required for proper chromosome segregation. This raises the possibility that a RITS-RDRC-like system operates in *C. elegans* to mediate the formation of specific chromatin structures that are essential for proper chromosome segregation. This notion is further supported by the observation by Claycomb et al., 2009 that CSR-1 is physically bound, in an RNA-dependent manner, to the chromosomal regions complementary to its associated siRNAs.

This analogy between the CSR-1 RNAi pathway in *C. elegans* and the RITS-RDRC model in *S. pombe*, may also explain the relatively weak phenotypic outcome in *cde-1* mutants, compared to *csr-1* and *ego-1* mutants. CSR-1 would be required to indicate the site of RITS action and without it, downstream players will not be able to localize and perform their function. Lack of EGO-1 would also lead to severe defects due to a total loss of siRNAs. (Note, however, that EGO-1 acts redundantly with the RdRP RRF-1 in other germline RNAi pathways as well (Gu et al., 2009), making the EGO-1 phenotype in this respect potentially more difficult to interpret.) In the model we propose, CDE-1 merely modifies the extent of siRNA accumulation. Therefore, its absence is expected to result in less severe defects compared to those observed in *csr-1* and *ego-1* mutants.

Besides similarities, differences between the *S. pombe* and a presumptive *C. elegans* RITS-RDRC systems are likely to exist. For example, in *S. pombe*, Rdp1 produces double stranded RNA that is subsequently processed by Dicer, whereas in *C. elegans* RdRP products appear to be directly bound by Argonautes (Aoki et al., 2007; Pak and Fire, 2007; Sijen et al., 2007), and are independent of Dicer (Gu et al., 2009). Another distinction between the two systems is the type of chromatin they appear to target: RITS-RDRC in *S. pombe* targets heterochromatin, whereas the CSR-1 pathway is associated with euchromatic regions (Claycomb et al., 2009).

Role of EGO-1, CDE-1 and CSR-1 in Chromosome Segregation

Our data suggest that chromosomal missegregation in *cde-1* mutant embryos may derive from improper chromosome

alignments that remain uncorrected during the course of the chromosome segregation process. What could be the molecular basis for this defect? As discussed above, mutation of *cde-1* triggers effects on transcript levels of many different genes, as determined by microarray analysis. Therefore, we cannot exclude the possibility that some of these changes play a role in establishing the observed chromosome segregation phenotype. However, given the facts that loss of the CDE-1 associated Argonaute, CSR-1, does not result in significant changes in transcript levels (Claycomb et al., 2009) and that the proteins in this specific RNAi pathway (CSR-1, EGO-1, CDE-1) all are physically associated with chromosomes in a centromere-like manner, we propose that the effect of this RNAi pathway on chromosome alignment is more direct. Analogous to findings in *S. pombe*, the CSR-1 RNAi pathway may directly influence the structure of pericentromeric regions, thereby affecting the function of the centromeric regions during mitosis, which is to attach the chromosomes to the microtubules of the spindle. If centromeres do not form properly as rigid structures on opposite sides of the chromosome, merotelic or syntelic attachments are unavoidable, complicating the execution of the chromosome segregation process.

In *C. elegans*, this process of obtaining correct spindle attachments may be more complex than in most other organisms as chromosomes are holocentric (Albertson and Thomson, 1982), meaning that centromeres are not confined to a distinct patch, but instead span the entire length of the condensed chromosome (reviewed in Dernburg, 2001; Maddox et al., 2004). Thus, defects in centromere function may lead to chromosomes that are less rigid over their entire length and cause them to twist along their axis, further complicating the formation of correct bipolar spindle attachments (Stear and Roth, 2002). Intriguingly, one of the commonly observed CENP-A figures in *cde-1* mutant metaphase plates resembles a twisted conformation, possibly originating from one or more individually twisted chromosomes of which the ends of each sister-chromatid have become attached to opposite sides of the spindle. We note, however, that higher resolution analysis will be required to further define the chromosome segregation defects in CSR-1 pathway mutants at the level of individual chromosomes. In addition, more detailed knowledge on the exact nature of centromeric DNA sequences and a better description of the molecular effects of the CSR-1 pathway will be essential to fully understand the link between RNAi and chromosome segregation in *C. elegans*.

Evolutionary Conservation

As the CDE-1 protein is well conserved throughout the animal kingdom, its role in RNAi or other RNA-based processes may also be conserved in other species, especially now RdRP activity has also been detected in mammalian cells (Maida et al., 2009). Furthermore, CDE-1-like proteins may be associated with the Piwi pathway. Somewhat analogous to RdRP-mediated amplification of small RNAs, Piwi proteins also generate an amplification cycle of small RNAs (piRNAs) (Brennecke et al., 2007; Gunaawardane et al., 2007). Interestingly, piRNAs carry a 2' Ome modification at their 3' ends (Horwich et al., 2007; Houwing et al., 2007), which inhibits nucleotidyltransferase activity (Li et al., 2005), suggesting that terminal transferase activity is rele-

vant in the Piwi pathway. Finally, proteins like CDE-1 may be involved in modifying miRNA expression post-transcriptionally. For example, processing of pre-*let-7* is regulated through uridylation (Heo et al., 2008), and a CDE-1-like enzyme was recently found to be responsible for this phenomenon (Heo et al., 2009). Thus, regulation of small RNA stability through modification of their 3' ends may turn out to be a widespread phenomenon.

EXPERIMENTAL PROCEDURES

Extensive descriptions of the methods and the microarray data (GEO accession number GSE18202) can be found in the [Supplemental Data](#).

Immunocytochemistry

For staining of RAD-51, HTP-3 and CDE-1, germlines or embryos were extruded in Egg Salts Buffer containing 0.1% Tween-20, followed by brief fixation in 2% formaldehyde. Samples were mounted on poly-lysine coated slides, permeabilised by freeze crack and fixed for one minute in -20°C methanol. Slides were washed in PBS containing 0.1% Tween-20 (PBST), and blocked in PBST with 5% lamb serum. First and second antibody incubations were performed overnight at 4°C and 3 hr at room temperature respectively. Slides were counterstained with DAPI.

For staining of CENP-A, CENP-F, and tubulin, embryos were extruded as described above, mounted and permeabilised by freeze crack followed by a 20 min -20°C methanol fixation. Washing and antibody incubations were performed as described above.

FISH

Germline or embryo slides were prepared as described above. Slides were washed in PBST, and gradually transferred to 100% ethanol. Slides were air-dried and preincubated in $2\times$ SSC 50% formamide at 37°C for 1 hr. The probe solution was sealed on the slide, and DNA was denatured at 95°C for 3 min, followed by hybridization overnight at 37°C . Slides were washed in $2\times$ SSC 50% formamide, $2\times$ SSC, $1\times$ SSC, and PBST, consecutively. Slides were counterstained with DAPI.

Video Microscopy

Embryos were extruded by dissection and mounted on 5% agarose pads in Egg Salts Buffer. Alternatively, hermaphrodites paralysed in Egg Salts buffer containing 0.5mM levamisole and 0.025% tricaine, were mounted on 5% agarose pads and embryos were imaged while inside the uterus. Images of DIC and GFP signals were captured every 10 s on a Leica microscope under the LasAF software.

Small RNA Cloning

Worms were staged as young adults, lysed by Protease K treatment and RNA was isolated using Trizol (Invitrogen). RNA was treated with Tobacco Acid Pyrophosphatase and subsequently poly(A)-tailed followed by ligation of a RNA adaptor to the 5'-phosphate of the small RNAs. First-strand cDNA synthesis was performed using an oligo(dT)-linker primer and M-MLV-RNase H- reverse transcriptase. cDNA was PCR-amplified for 16 cycles according to instructions of Illumina/Solexa. cDNA was size selected on a preparative 6% polyacrylamide (PAA) gel. The eluted cDNA was sent for sequencing on an Illumina/Solexa platform. Libraries made from CSR-1 IPs were made without polyA tailing. See supplemental material for a detailed description. Sequencing data has been submitted at GEO, accession number GSE17787.

Sequence Analysis

Adaptor sequences were trimmed from generated data using custom scripts. Resulting inserts were mapped to the *C. elegans* genome (ce4) using the megablast program (Zhang et al., 2000), and genomic annotations of mapped reads were retrieved from the Ensembl database (release 52, dec 2008) using Perl API provided by Ensembl (Hubbard et al., 2007). Read counts for the different annotated classes are listed in [Table S2](#). Sequences will be made

available upon publication. Normalization issues regarding these libraries are discussed in the [Supplemental Data](#).

SUPPLEMENTAL DATA

Supplemental Data include Supplemental Results, Supplemental Discussion, Supplemental Experimental Procedures, Supplemental References, eleven figures, two tables, and seven movies and can be found with this article online at [http://www.cell.com/supplemental/S0092-8674\(09\)01172-6](http://www.cell.com/supplemental/S0092-8674(09)01172-6).

ACKNOWLEDGMENTS

We thank Abby Dernburg and members of her lab for protocols, reagents and support concerning the immunostainings and microscopy. We thank Alex Dammermann, Karen Oegema, Reto Gassmann, and Arshad Desai for antibodies and transgenic strains. Several strains were generously provided by the *Caenorhabditis* Genetics Center (CGC), by Shohei Mitani of the Japanese National Bioresources Project for *C. elegans* and Hendrik Korswagen. PGL-1 antibody (OIC104) was provided by the Developmental Studies Hybridoma Bank (DSHB). This work was supported by the National Proteomics Centre, the European Union Sixth Framework Program Integrated Project SIROCCO (Grant LSHG-CT-2006-037900), VIDI fellowships from the Netherlands Organisation for Scientific Research (NWO; R.F.K. and E.B.) and an ERC Starting Grant from the Ideas Program of the European Union Seventh Framework Program (R.F.K.; Grant 202819).

Received: March 9, 2009

Revised: July 1, 2009

Accepted: September 11, 2009

Published: October 1, 2009

REFERENCES

- Albertson, D.G., and Thomson, J.N. (1982). The kinetochores of *Caenorhabditis elegans*. *Chromosoma* **86**, 409–428.
- Aoki, K., Moriguchi, H., Yoshioka, T., Okawa, K., and Tabara, H. (2007). In vitro analyses of the production and activity of secondary small interfering RNAs in *C. elegans*. *EMBO J.* **26**, 5007–5019.
- Beanan, M.J., and Strome, S. (1992). Characterization of a germ-line proliferation mutation in *C. elegans*. *Development* **116**, 755–766.
- Brennecke, J., Aravin, A.A., Stark, A., Dus, M., Kellis, M., Sachidanandam, R., and Hannon, G.J. (2007). Discrete small RNA-generating loci as master regulators of transposon activity in *Drosophila*. *Cell* **128**, 1089–1103.
- Buchwitz, B.J., Ahmad, K., Moore, L.L., Roth, M.B., and Henikoff, S. (1999). A histone-H3-like protein in *C. elegans*. *Nature* **401**, 547–548.
- Buhler, M., Spies, N., Bartel, D.P., and Moazed, D. (2008). TRAMP-mediated RNA surveillance prevents spurious entry of RNAs into the Schizosaccharomyces pombe siRNA pathway. *Nat. Struct. Mol. Biol.* **15**, 1015–1023.
- Chen, C.C., Simard, M.J., Tabara, H., Brownell, D.R., McCollough, J.A., and Mello, C.C. (2005). A member of the polymerase beta nucleotidyltransferase superfamily is required for RNA interference in *C. elegans*. *Curr. Biol.* **15**, 378–383.
- Claycomb, J.M., Batista, P.J., Pang, K.M., Gu, W., Vasale, J.J., van Wolfswinkel, J.C., Chaves, D.A., Shirayama, M., Mitani, S., Ketting, R.F., Conte, D., Jr., and Mello, C.C. (2009). The Argonaute CSR-1 and its 22G-RNA cofactors target germline genes and are required for holocentric chromosome segregation. *Cell* **139**, this issue, 123–134.
- Crittenden, S.L., Eckmann, C.R., Wang, L., Bernstein, D.S., Wickens, M., and Kimble, J. (2003). Regulation of the mitosis/meiosis decision in the *Caenorhabditis elegans* germline. *Philos. Trans. R. Soc. Lond. B Biol. Sci.* **358**, 1359–1362.
- Dernburg, A.F. (2001). Here, there, and everywhere: kinetochore function on holocentric chromosomes. *J. Cell Biol.* **153**, F33–F38.
- Ekwall, K. (2004). The roles of histone modifications and small RNA in centromere function. *Chromosome Res.* **12**, 535–542.
- Fire, A., Xu, S., Montgomery, M.K., Kostas, S.A., Driver, S.E., and Mello, C.C. (1998). Potent and specific genetic interference by double-stranded RNA in *Caenorhabditis elegans*. *Nature* **391**, 806–811.
- Folco, H.D., Pidoux, A.L., Urano, T., and Allshire, R.C. (2008). Heterochromatin and RNAi are required to establish CENP-A chromatin at centromeres. *Science* **319**, 94–97.
- Gassmann, R., Essex, A., Hu, J.S., Maddox, P.S., Motegi, F., Sugimoto, A., O'Rourke, S.M., Bowerman, B., McLeod, I., Yates, J.R., 3rd, et al. (2008). A new mechanism controlling kinetochore-microtubule interactions revealed by comparison of two dynein-targeting components: SPDL-1 and the Rod/Zwilch/Zw10 complex. *Genes Dev.* **22**, 2385–2399.
- Gu, W., Shirayama, M., Conte, D., Jr., Vasale, J., Batista, P.J., Claycomb, J.M., Moresco, J.J., Youngman, E., Keys, J., Stoltz, M.J., et al. (2009). Distinct Argonaute-mediated 22G-RNA pathways direct genome surveillance in the *C. elegans* germline. *Mol. Cell*. Published online October 1, 2009. 10.1016/j.molcel.2009.09.020.
- Gunawardane, L.S., Saito, K., Nishida, K.M., Miyoshi, K., Kawamura, Y., Nagami, T., Siomi, H., and Siomi, M.C. (2007). A slicer-mediated mechanism for repeat-associated siRNA 5' end formation in *Drosophila*. *Science* **315**, 1587–1590.
- Hall, I.M., Noma, K., and Grewal, S.I. (2003). RNA interference machinery regulates chromosome dynamics during mitosis and meiosis in fission yeast. *Proc. Natl. Acad. Sci. USA* **100**, 193–198.
- Heo, I., Joo, C., Cho, J., Ha, M., Han, J., and Kim, V.N. (2008). Lin28 mediates the terminal uridylation of let-7 precursor microRNA. *Mol. Cell* **32**, 276–284.
- Heo, I., Joo, C., Kim, Y., Ha, M., Yoon, M., Cho, J., Yeom, K., Han, J., and Kim, V.N. (2009). TUT4 in concert with Lin28 suppresses microRNA biogenesis through pre-microRNA uridylation. *Cell* **138**, 696–708.
- Horwich, M.D., Li, C., Matranga, C., Vagin, V., Farley, G., Wang, P., and Zamore, P.D. (2007). The *Drosophila* RNA methyltransferase, DmHen1, modifies germline piRNAs and single-stranded siRNAs in RISC. *Curr. Biol.* **17**, 1265–1272.
- Houwing, S., Kamminga, L.M., Berezikov, E., Cronembold, D., Girard, A., van den Elst, H., Filippov, D.V., Blaser, H., Raz, E., Moens, C.B., et al. (2007). A role for Piwi and piRNAs in germ cell maintenance and transposon silencing in Zebrafish. *Cell* **129**, 69–82.
- Hubbard, T.J., Aken, B.L., Beal, K., Ballester, B., Caccamo, M., Chen, Y., Clarke, L., Coates, G., Cunningham, F., Cutts, T., et al. (2007). Ensembl 2007. *Nucleic Acids Res.* **35**, D610–D617.
- Katoh, T., Sakaguchi, Y., Miyauchi, K., Suzuki, T., Kashiwabara, S., and Baba, T. (2009). Selective stabilization of mammalian microRNAs by 3' adenylation mediated by the cytoplasmic poly(A) polymerase GLD-2. *Genes Dev.* **23**, 433–438.
- Ketting, R.F., Haverkamp, T.H., van Luenen, H.G., and Plasterk, R.H. (1999). Mut-7 of *C. elegans*, required for transposon silencing and RNA interference, is a homolog of Werner syndrome helicase and RNaseD. *Cell* **99**, 133–141.
- Kim, S.K., Lund, J., Kiraly, M., Duke, K., Jiang, M., Stuart, J.M., Eizinger, A., Wylie, B.N., and Davidson, G.S. (2001). A gene expression map for *Caenorhabditis elegans*. *Science* **293**, 2087–2092.
- Kwak, J.E., and Wickens, M. (2007). A family of poly(U) polymerases. *RNA* **13**, 860–867.
- Li, J., Yang, Z., Yu, B., Liu, J., and Chen, X. (2005). Methylation protects miRNAs and siRNAs from a 3'-end uridylation activity in *Arabidopsis*. *Curr. Biol.* **15**, 1501–1507.
- Maddox, P.S., Oegema, K., Desai, A., and Cheeseman, I.M. (2004). "Holo"er than thou: chromosome segregation and kinetochore function in *C. elegans*. *Chromosome Res.* **12**, 641–653.
- Maida, Y., Yasukawa, M., Furuuchi, M., Lassmann, T., Possemato, R., Okamoto, N., Kasim, V., Hayashizaki, Y., Hahn, W.C., and Masutomi, K. (2009). An RNA-dependent RNA polymerase formed by TERT and the RMRP RNA. *Nature*, doi:10.1038.

- Martienssen, R.A., Zaratiegui, M., and Goto, D.B. (2005). RNA interference and heterochromatin in the fission yeast *Schizosaccharomyces pombe*. *Trends Genet.* *21*, 450–456.
- Mello, C.C., and Conte, D., Jr. (2004). Revealing the world of RNA interference. *Nature* *431*, 338–342.
- Moore, L.L., Morrison, M., and Roth, M.B. (1999). HCP-1, a protein involved in chromosome segregation, is localized to the centromere of mitotic chromosomes in *Caenorhabditis elegans*. *J. Cell Biol.* *147*, 471–480.
- Motamedj, M.R., Verdell, A., Colmenares, S.U., Gerber, S.A., Gygi, S.P., and Moazed, D. (2004). Two RNAi complexes, RITS and RDRC, physically interact and localize to noncoding centromeric RNAs. *Cell* *119*, 789–802.
- Olsen, A., Vantipalli, M.C., and Lithgow, G.J. (2006). Checkpoint proteins control survival of the postmitotic cells in *Caenorhabditis elegans*. *Science* *312*, 1381–1385.
- Pak, J., and Fire, A. (2007). Distinct populations of primary and secondary effectors during RNAi in *C. elegans*. *Science* *315*, 241–244.
- Reinke, V., Gil, I.S., Ward, S., and Kazmer, K. (2004). Genome-wide germline-enriched and sex-biased expression profiles in *Caenorhabditis elegans*. *Development* *131*, 311–323.
- Reinke, V., Smith, H.E., Nance, J., Wang, J., Van Doren, C., Begley, R., Jones, S.J., Davis, E.B., Scherer, S., Ward, S., et al. (2000). A global profile of germline gene expression in *C. elegans*. *Mol. Cell* *6*, 605–616.
- Rissland, O.S., Mikulasova, A., and Norbury, C.J. (2007). Efficient RNA polyuridylation by noncanonical poly(A) polymerases. *Mol. Cell Biol.* *27*, 3612–3624.
- Rissland, O.S., and Norbury, C.J. (2009). Decapping is preceded by 3' uridylation in a novel pathway of bulk mRNA turnover. *Nat. Struct. Mol. Biol.*
- Robert, V.J., Sijen, T., van Wolfswinkel, J., and Plasterk, R.H. (2005). Chromatin and RNAi factors protect the *C. elegans* germline against repetitive sequences. *Genes Dev.* *19*, 782–787.
- Schmid, M., Kuchler, B., and Eckmann, C.R. (2009). Two conserved regulatory cytoplasmic poly(A) polymerases, GLD-4 and GLD-2, regulate meiotic progression in *C. elegans*. *Genes Dev.* *23*, 824–836.
- Sijen, T., and Plasterk, R.H. (2003). Transposon silencing in the *Caenorhabditis elegans* germline by natural RNAi. *Nature* *426*, 310–314.
- Sijen, T., Steiner, F.A., Thijssen, K.L., and Plasterk, R.H. (2007). Secondary siRNAs result from unprimed RNA synthesis and form a distinct class. *Science* *315*, 244–247.
- Smardon, A., Spoerke, J.M., Stacey, S.C., Klein, M.E., Mackin, N., and Maine, E.M. (2000). EGO-1 is related to RNA-directed RNA polymerase and functions in germ-line development and RNA interference in *C. elegans*. *Curr. Biol.* *10*, 169–178.
- Stear, J.H., and Roth, M.B. (2002). Characterization of HCP-6, a *C. elegans* protein required to prevent chromosome twisting and merotelic attachment. *Genes Dev.* *16*, 1498–1508.
- Tabara, H., Sarkissian, M., Kelly, W.G., Fleenor, J., Grishok, A., Timmons, L., Fire, A., and Mello, C.C. (1999). The rde-1 gene, RNA interference, and transposon silencing in *C. elegans*. *Cell* *99*, 123–132.
- Verdel, A., Jia, S., Gerber, S., Sugiyama, T., Gygi, S., Grewal, S.I., and Moazed, D. (2004). RNAi-mediated targeting of heterochromatin by the RITS complex. *Science* *303*, 672–676.
- Wang, L., Eckmann, C.R., Kadyk, L.C., Wickens, M., and Kimble, J. (2002). A regulatory cytoplasmic poly(A) polymerase in *Caenorhabditis elegans*. *Nature* *419*, 312–316.
- Win, T.Z., Stevenson, A.L., and Wang, S.W. (2006). Fission yeast cid12 has dual functions in chromosome segregation and checkpoint control. *Mol. Cell Biol.* *26*, 4435–4447.
- Yigit, E., Batista, P.J., Bei, Y., Pang, K.M., Chen, C.C., Tolia, N.H., Joshua-Tor, L., Mitani, S., Simard, M.J., and Mello, C.C. (2006). Analysis of the *C. elegans* Argonaute family reveals that distinct Argonautes act sequentially during RNAi. *Cell* *127*, 747–757.
- Zhang, Z., Schwartz, S., Wagner, L., and Miller, W. (2000). A greedy algorithm for aligning DNA sequences. *J. Comput. Biol.* *7*, 203–214.